Synthesis, Characterization, and Oxygenation of Bis-fenced Porphyrinato Iron(II) and Cobalt(II) Complexes†

Eishun Tsuchida,* Teruyuki Komatsu, Etsuo Hasegawa, and Hiroyuki Nishide
Department of Polymer Chemistry, Waseda University, Tokyo 169, Japan

The both-faces-hindered and highly symmetric complexes 5,10,15,20-tetra(2',6'-dipivaloyloxyphenyl)porphyrinato-iron(II) and -cobalt(II), which have no amide residues but ester ones in the fence groups, have been synthesized. The iron(II) complex formed stable and reversible dioxygen adducts in toluene at 25 °C. The half-life for irreversible oxidation is longer than 1 d. The ligation properties for this complex with imidazole derivatives or dioxygen have been determined and compared to those of one-face-hindered porphyrinatoiron complexes. The bulky groups on both sides of the macrocycle decrease the binding constants for imidazole and for dioxygen. The binding characteristics of an imidazole derivative, which is sterically restrained by the bulky groups, have been clarified by Mössbauer and i.r. spectroscopic measurements. A kinetic study of dioxygen association and dissociation suggests that the low oxygen affinity is brought about primarily by the high rate of ligand dissociation.

Models of dioxygen carriers have been prepared and discussed in order to understand the nature of the binding of dioxygen or carbon monoxide to haemoglobin (hb) and myoglobin (mb).[1–8] Much attention in recent years has been paid to iron complexes of substituted tetraphenylporphyrin derivatives.[1–3,5,6] Such highly modified porphyrinatoiron derivatives have different electronic or steric environments around the dioxygen binding sites on a single face or both faces of the porphyrin plane and form dioxygen adducts reversibly only at low temperature. Several successful models involve an appropriate pocket on the ring plane and bind dioxygen reversibly at 25 °C, and the dioxygen adducts are stable against irreversible oxidation.[1,3,5] Typical of these are the 'picket-fence porphyrins' and 'pocket porphyrins', the iron(II) complexes of which can bind dioxygen reversibly in toluene solution containing an excess of axial base at 25 °C.[1] However, these single-face hindered porphyrin complexes are irreversibly oxidized rapidly by dioxygen under conditions where the axial base concentration is very low. Therefore, it is necessary to modify the rear side of the porphyrin plane to prevent irreversible oxidation by the dimerization of haems through the unhindered side. The 'basket-handle porphyrins',[3] 'bis-pocket porphyrins',[5] and 'doubly bridged porphyrins'[7] are suitable model compounds having both faces hindered, and have very interesting properties for dioxygen binding. However, the preparation of such derivatives is generally not easy and the yield rather low. It is expected from the standpoint of synthesis that the construction of the same bulky groups on both sides of the porphyrin plane would be very easy, because it would remove all the problems concerning undesired atropisomers of substituted tetraphenylporphyrins.

It is well known that the apoproteins of hb and mb make protohaems bind dioxygen reversibly and the dioxygen adducts stable against irreversible oxidation through a proton-driven process. *X*-Ray structural analyses of oxyhaemoglobin have provided direct evidence that the dioxygen ligand forms a hydrogen bond with the distal histidine (His E7).[9] On the other hand, many of the models, derived from *meso*-tetra(aminophenyl)porphyrin, have amide residues in the hydrophobic pocket on the porphyrin plane and these amide groups were suggested to interact with bound dioxygen.[1,3,6]

Oxygen-17 n.m.r. spectra of the Fe–O_2 moiety of 'single-face hindered porphyrins' have recently demonstrated the hydrogen bonding and long-range dipole–dipole interaction of the bound dioxygen with amide residues of the handle anchoring groups.[10] Further, by the study of a series of 'hanging-base porphyrins', it was found that amide handle derivatives had an affinity for dioxygen larger than that of ether handle ones.[3]

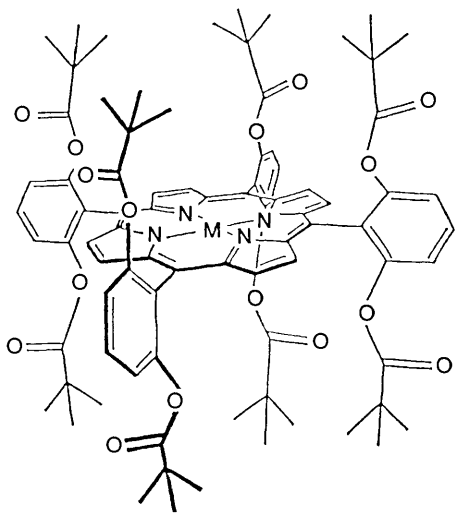

	M
(**3a**)	$2H^+$
(**3b**)	Fe^{2+}
(**3b'**)	Fe^{3+}
(**3c**)	Co^{3+}

In view of the great importance of these two points, it is interesting to design a new type of model compound which has bulky fences with no amide residues but an ester one on both sides of the porphyrin ring plane. We designed and synthesized the highly symmetric and bis-fenced complexes 5,10,15,20-tetra(2',6'-dipivaloyloxyphenyl)porphyrinato-iron(II) (**3b**) and -cobalt(II) (**3c**).[11] Their characteristic ligation properties with imidazole derivatives or gaseous ligand (O_2 or CO) have been clarified by various physicochemical measurements.

† *Non-S.I. units employed:* mmHg ≈ 133 Pa, cal = 4.184 J.

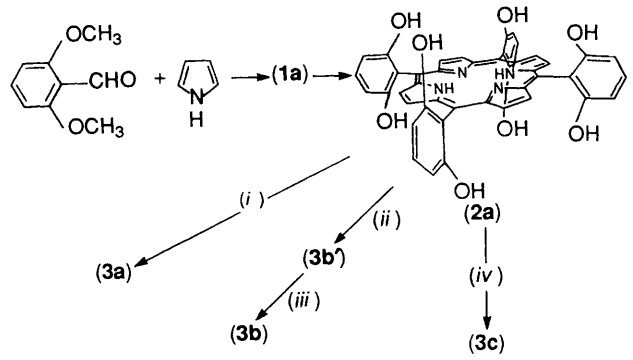

Scheme. (*i*) $(CH_3)_3CCOCl$; (*ii*) (*a*) $FeBr_2$, (*b*) $(CH_3)_3CCOCl$; (*iii*) $Na_2S_2O_4$; (*iv*) (*a*) $CoCl_2$, (*b*) $(CH_3)_3CCOCl$

Experimental

General.—Infrared spectra were recorded with a JASCO IR-880 spectrometer, ^1H n.m.r. (400 MHz) and ^{13}C n.m.r. (100 MHz) spectra on a JEOL GSX-400 instrument. Chemical shifts are expressed in p.p.m. downfield from $SiMe_4$ as an internal standard. Fast atom bombardment mass spectra were measured with a JEOL DX-303 spectrometer. Elemental analyses were performed on a Yanagimoto MT3 CHN corder. Thin-layer chromatography (t.l.c.) was carried out on 0.2-mm precoated plates of silica gel 60 F-254 (Merck). Purification of products was performed by silica gel 60 (Merck) column chromatography. Solvents were evaporated with a type-N2 Tokyo Rikakikai rotary evaporator.

Materials and Solvents.—Pyrrole, 1-methylimidazole (mim), and 1,2-dimethylimidazole (dmim) were purified before use by distillation *in vacuo* under reduced pressure. 2,6-Dimethoxybenzaldehyde, propionic acid, boron tribromide, pivaloyl chloride, and 4-(dimethylamino)pyridine are commercially available as special grade and were used without further purification. Tetrahydrofuran (thf), toluene, and benzene were purified immediately before use by distillation from sodium and benzophenone under argon. Dichloromethane (CH_2Cl_2) was purified before use by distillation from calcium hydride under nitrogen.

The synthetic route to complexes (**3b**) and (**3c**) is shown in the Scheme.

5,10,15,20-*Tetra*(2′,6′-*dimethoxyphenyl*)*porphyrin* (**1a**). 2,6-Dimethoxybenzaldehyde (10 g, 60.2 mmol) was dissolved in propionic acid (500 cm^3). The solution was then heated to 100—120 °C with continuous stirring. Pyrrole (4.18 cm^3, 60.2 mmol) was slowly added to the heated solution and the heating was continued at 100—120 °C for 7 h. After the solution had cooled to room temperature it was left to stand overnight. The purple crystalline products were isolated by suction filtration and washed well with MeOH until the washings were essentially colourless. The crude product was recrystallized from CH_2Cl_2–MeOH and dried at room temperature for several hours *in vacuo* to give purple crystalline (**1a**) (1.6 g, 12.4%); R_f 0.60 (CH_2Cl_2). $\delta_H(CDCl_3)$ −2.8 (2 H, s, inner H), 3.5 (24 H, s, OCH_3), 7.2—7.8 (12 H, m, phenyl H), and 8.8 (8 H, s, pyrrole H). I.r. (KBr): 1 280 cm^{-1} [ν(COC)]. $\lambda_{max.}(CH_2Cl_2)$: 645, 586, 542, 511, and 414 nm.

5,10,15,20-*Tetra*(2′,6′-*dihydroxyphenyl*)*porphyrin* (**2a**). Compound (**1a**) (1.6 g, 1.87 mmol) was dissolved in dry CH_2Cl_2 (100 cm^3) at −20 °C, followed by the addition of BBr_3 (1.77 cm^3, 18.7 mmol). The resulting green solution was stirred for 12 h, then cautiously placed in ice–water. Ethyl acetate (200 cm^3) was added to the suspension and the mixture neutralized with $NaHCO_3$. The organic layer was separated, washed first with dilute aqueous HCl then twice with water, and dried over anhydrous sodium sulphate. The solution was reduced to small volume on a rotary evaporator and residue chromatographed on a dry silica gel column using ethyl acetate–MeOH (20:1, v/v) as the eluant, giving compound (**2a**) (1.04 g, 75.2%); R_f 0.80 (ethyl acetate–MeOH, 20:1 v/v). $\delta_H(CD_3OD)$ −2.7 (2 H, s, inner H), 7.2—7.8 (12 H, m, phenyl H), and 8.8 (8 H, s, pyrrole H). I.r. (KBr): 3 350 cm^{-1} [ν(OH)]. $\lambda_{max.}$(MeOH) 641, 586, 544, 511, and 414 nm.

Iron insertion. Compound (**2a**) (1 g, 1.35 mmol) and anhydrous iron(II) bromide (7.98 g, 27 mmol) were dissolved in dry thf (200 cm^3) and the mixture heated to reflux under nitrogen. The reaction was complete after 6 h. The mixture was then brought to dryness on a rotary evaporator, extracted with ethyl acetate and the resulting solution chromatographed on a dry silica gel column using ethyl acetate–MeOH (20:1 v/v) as the eluant. The eluate was treated with concentrated HBr (0.2 cm^3) and dried at room temperature for several hours *in vacuo*, to give a dark purple crystalline iron(III) complex (**2b**) (1.0 g, 84.1%); R_f 0.60 (ethyl acetate–MeOH, 20:1 v/v). I.r. (KBr): 3 350 cm^{-1} [ν(OH)]. $\lambda_{max.}$(MeOH) 674, 640, 575, 504, and 414 nm.

Cobalt insertion. Compound (**2a**) (1 g, 1.35 mmol), 2,6-dimethylpyridine (0.47 cm^3, 4.05 mmol), and anhydrous cobalt(II) chloride (1.4 g, 10.8 mmol) were dissolved in dry thf (200 cm^3) and heated to reflux under nitrogen. The reaction was complete after 2 h. The mixture was then brought to dryness on a rotary evaporator, extracted with ethyl acetate and the resulting solution chromatographed on a dry silica gel column using ethyl acetate–MeOH (20:1 v/v) as the eluant. The eluate was reduced to small volume on a rotary evaporator and the residue dried at room temperature for several hours *in vacuo*, to give a purple crystalline product (**2c**) (0.98 g, 90.9%); R_f 0.60 (ethyl acetate–MeOH, 20:1 v/v). I.r. (KBr): 3 350 cm^{-1} [ν(OH)]. $\lambda_{max.}$(MeOH) 553, 522, and 405 nm.

5,10,15,20-*Tetra*(2′,6′-*dipivaloyloxyphenyl*)*porphyrin* (**3a**). Pivaloyl chloride (1.66 cm^3, 13.5 mmol) and 4-(dimethylamino)-pyridine (1.65 g, 13.5 mmol) were added to a dry thf solution (100 cm^3) of compound (**2a**) (1 g, 1.35 mmol). The mixture was stirred for 10 h at 25 °C under nitrogen, then brought to dryness on a rotary evaporator and extracted with dichloromethane. The organic layer was washed, first with dilute HCl and then with aqueous ammonia. The resulting solution was evaporated on a rotary evaporator and the residue chromatographed on a dry silica gel column using $CHCl_3$–diethyl ether (10:1 v/v) as the eluant. The eluate was reduced to small volume on a rotary evaporator and the residue dried at room temperature for several hours *in vacuo*, to give a purple crystalline product (**3a**) (1.17 g, 61.4%); R_f 0.53 ($CHCl_3$–diethyl ether, 10:1 v/v) (Found: C, 67.65; H, 7.15; N, 3.50; M^+, 1 415. $C_{84}H_{94}N_4O_{16}\cdot 4H_2O$ requires C, 67.80; H, 6.90; N, 3.75%, M^+ = 1 415.7). For further microanalyses, a small amount of the compound was dried *in vacuo* at 60 °C for 1 d (Found: C, 71.25; H, 6.70; N, 3.95%). $\delta_H(CDCl_3)$ −2.8 (2 H, s, inner H), −0.3 (72 H, s, pivaloyl), 7.4—7.9 (12 H, m, phenyl H), and 8.8 (8 H, s, pyrrole β-H); $\delta_C(CDCl_3)$ 25.7 (methyl), 38.0 (quaternary carbon), 109.0 (*meso*), 131.2 (pyrrole β-carbon), 146.9 (pyrrole α-carbon), 120.2, 128.2, 129.6, 151.8 (phenyl), and 175.5 p.p.m. (carbonyl). I.r. (KBr): 1 760 cm^{-1} [ν(CO)]. $\lambda_{max.}(CHCl_3)$ 637, 583, 536, 507, and 412 nm.

5,10,15,20-*Tetra*(2′,6′-*dipivaloyloxyphenyl*)*porphyrinato-iron*(III) *bromide* (**3b′**) *and -cobalt*(II) (**3c**). Complexes (**3b′**) and (**3c**) were obtained from the compound (**2a**) by use of pivaloyl chloride and the appropriate metal(II) chloride. Finally, purple crystalline products (**3b′**) (1.23 g, 58.9%) and (**3c**) (1.14 g, 57.1%) were obtained. Complex (**3b′**): R_f 0.55 $CHCl_3$–diethyl ether, 10:1 v/v) (Found: C, 66.20; H, 6.60; N, 3.30; M^+ 1 549. $C_{84}H_{92}BrFeN_4O_{16}\cdot H_2O$ requires C, 66.25; H, 6.20; N, 3.70%).

I.r. (KBr): 1 760 cm^{-1} [ν(CO)]. $\lambda_{max.}(CHCl_3)$ 680, 650, 579, 508, and 416 nm. Complex (**3c**): R_f 0.50 ($CHCl_3$–diethyl ether, 10:1 v/v) (Found: C, 68.10; H, 6.75; N, 3.45; M^+ 1 472. $C_{84}H_{92}CoN_4O_{16}\cdot H_2O$ requires C, 67.70; H, 6.35; N, 3.75%). I.r. (KBr): 1 760 cm^{-1} [ν(CO)]. $\lambda_{max.}(CHCl_3)$ 553, 522, and 404 nm. The iron 57-labelled derivative of (**3b'**), used for Möessbauer spectroscopic measurement, was also synthesized according to the above method.

Iron(II) *complex.* Complex (**3b'**) (0.15 g, 0.1 μmol) was dissolved in toluene (5 cm^3) and the solution purged with argon to remove any oxygen. Then deoxygenated aqueous $Na_2S_2O_4$ solution (5 cm^3) was added. The mixture was vigorously stirred for 1 h, the red-orange organic layer collected and dried over anhydrous Na_2SO_4. After filtration from Na_2SO_4 under argon, a toluene solution of a four-co-ordinated iron(II) porphyrin (**3b**) (20 μmol dm^{-3}) was obtained.

1-*Hexylimidazole* (him). This compound was synthesized as reported previously.[7]

Base Equilibrium Measurement.—Equilibrium constants of the bases were determined at 25 °C under argon by titration of the four-co-ordinated metalloporphyrins ML (M = Fe or Co) with aliquots of an imidazole derivative dissolved in deoxygenated toluene. For the bases there are two possible equilibria, (1) and (2). When $K_B^B = 0$ the titration shows isosbestic points

$$ML + B \rightleftharpoons ML\cdot B \quad (1)$$

$$ML\cdot B + B \rightleftharpoons ML\cdot 2B \quad (2)$$

and the data can be fitted to the Drago equation.[12] When the three species ML, ML·B, and ML·2B are present simultaneously, K^B and K_B^B can be calculated by using the Brault and Rougee equations.[13] The temperature of the solution was maintained to a precision of ±0.2 °C. In general, metalloporphyrin concentrations of 20—30 μmol dm^{-3} were used, and spectra were recorded in the range 550—350 nm by use of a Shimazu UV-2100 high-sensitive spectrophotometer equipped with a thermostatted cell holder.

Dioxygenation of Metalloporphyrins.—Dioxygenation of metalloporphyrins can be expressed by equation (3). The

$$ML\cdot B + O_2 \rightleftharpoons ML\cdot B\cdot O_2 \quad (3)$$

oxygen-binding affinity (oxygen pressure at half oxygen binding for the metalloporphyrin, $P_{50} = 1/K_B^{O_2}$) was determined from the spectral changes at various partial pressures of dioxygen. The corresponding thermodynamic parameters (ΔH, ΔS) were calculated by measurement of the oxygen-binding affinity at various temperatures, using van't Hoff plots. The temperature of the solution was maintained to a precision of ±0.2 °C. In general, metalloporphyrin concentrations of 20—30 μmol dm^{-3} were used, and spectra were recorded in the range 650—350 nm. The low temperature measurements were performed using a cell mounted in a Dewar vessel.

Kinetic Measurements.—Kinetic measurements were performed by monitoring the transmittance of a solution subjected to a pulse of photolyzing light. Oxygen-binding rate constants ($k_B^{O_2}$, $k_B^{-O_2}$) were determined by pseudo-first-order kinetics at various partial pressures of dioxygen, using a Unisoku USP-500 flash-photolysis spectrophotometer. Haem concentrations of 10 μmol dm^{-3} were used, and the absorbance changes were monitored at 435 nm in toluene at 25 °C.

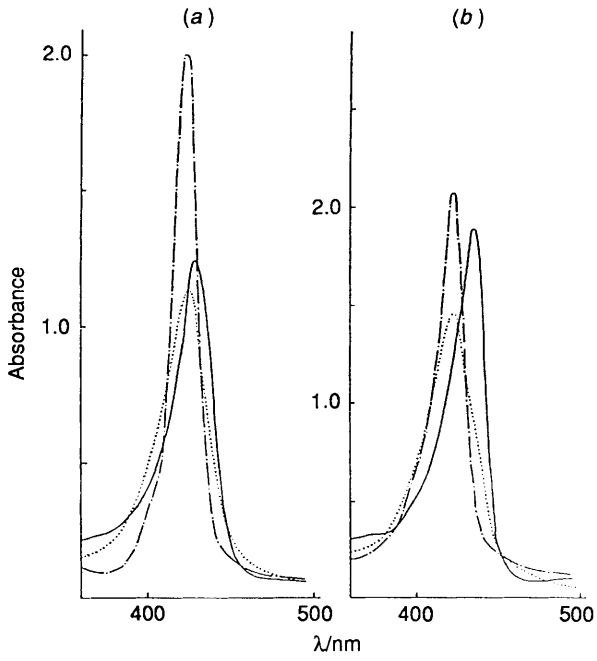

Figure 2. Visible absorption spectra of various forms of bis-fenced porphyrinatoiron(II) (20 μmol dm^{-3}) in toluene [deoxy (——), O_2 adduct (· · · · ·), and CO adduct (— · — · —)]: (*a*) (**3b**)·mim at 25 °C; (*b*) (**3b**)·dmim at −20 °C

Infrared Spectroscopy.—The i.r. differential spectra were measured under $^{16}O_2$ *vs.* $^{18}O_2$ and $^{12}C^{16}O$ *vs.* nitrogen atmospheres. The haem concentration was 10 mmol dm^{-3} in benzene, and the cells used were precisely matched in terms of path length (0.1 mm) and NaCl window thickness. The spectra were recorded with a double-beam type spectrometer in absorbance mode.

Mössbauer Spectroscopy.—The Mössbauer spectra were recorded under argon, CO, or O_2, respectively, at 77 K. The spectrometer was of the constant-acceleration type, the source consisted of *ca.* 10 mCi (3.7×10^8 Bq) of ^{57}Co-diffused palladium foil, and the absorber (thickness *ca.* 0.2 mg of iron per cm^2) was kept at 77 K. The Doppler velocity was calibrated with natural iron foil kept at 25 °C, and zero velocity was taken as the centroid of its spectrum at 25 °C. The spectra were fitted by Lorentzian line shapes using a least-squares program.

Results

The equilibrium constants (K^B, K_B^B) were obtained by spectrophotomeric titrations of toluene solutions of metal(II) porphyrin complexes with base under an argon atmosphere. The addition of dmim to (**3b**) and mim to (**3c**) gives only five-co-ordinate species [equation (1)] and well defined isosbestic points are observed in the visible absorption spectra during titration. The data can be fitted by Drago's equation.[12] When the less-hindered base mim is used, (**3b**) forms a six-co-ordinate species [equation (2)]. The spectroscopic data were analyzed by the mathematical method described by Brault and Rougee.[13] Values for the equilibrium constants for base addition to complexes (**3b**) and (**3c**) are given in Table 1.

Spectrophotomeric dioxygen titrations of (**3b**)·mim, (**3b**)·dmim, and (**3c**)·mim were done under conditions of an excess of base. Isosbestic points were maintained in all titrations. The complex (**3b**)·mim formed a dioxygen adduct reversibly at 25 °C, which changed to the corresponding CO adduct on bubbling carbon monoxide gas through the solution.

Table 1. Ligation equilibria constants, oxygen-affinity and thermodynamic parameters for iron(II) and cobalt(II) porphyrin complexes in toluene at 25 °C

Porphyrin complex	Ligand	K_B/dm^3 mol^{-1}	K_B^B/dm^3 mol^{-1}	P_{50}/mmHg	ΔH/kcal mol^{-1}	ΔS/cal K^{-1} mol^{-1}
(3b)	mim	13	50	56	—	—
(3b)	dmim	36	—	866[a]	−9.3	−31
[Fe(tpp)][b]	Him	8.8×10^3	7.9×10^4	—	—	—
[Fe(tpvp)][c]	dmim	3.2×10^4	—	38	−14.3	−42
[Fe(ttpp)][d]	dmim	2.7×10^4	—	508	−14.4	−47
e	mim	1.5×10^5	—	1.0×10^{-1}	—	—
(3c)	mim	5	—	136[f]	—	—
[Co(tpvp)][g]	mim	1.7×10^4	—	140	−12.2	−38

[a] Calculated from thermodynamic values. [b] tpp = 5,10,15,20-tetraphenylporphyrinate, Him = imidazole. From ref. 13. [c] Ref. 14. [d] ttpp = 5,10,15,20-tetra(2,4,6-triphenylphenyl)porphyrinate. From ref. 5. [e] A 'basket-handle' derivative of 10,20-bis(*o*-pivalamidophenyl)porphyrinatoiron(II). From ref. 3. [f] In CH_2Cl_2 at −66 °C. [g] From ref. 19.

Table 2. *Oxygen-binding* rates and equilibrium constants for iron(II) porphyrin complexes in toluene at 25 °C

Haem	Ligand	$10^{-7}k_B^{O_2}$/dm^3 mol^{-1} s^{-1}	$k_B^{-O_2}$/s^{-1}	$K_B^{O_2}$/dm^3 mol^{-1}
(3b)	mim	2.3	6.6×10^3	3.4×10^3
Chelated[a]	—	6.2	4.2×10^3	1.5×10^4
Anthracene bridged[b]	dcim	6.5	1.0×10^3	6.5×10^4
Medium pocket[c]	mim	1.7	71	2.4×10^5

[a] Chelated protohaem II. From ref. 16. [b] Derivative of (di-n-butyl 3,8,13,18-tetramethylporphyrin-2,12-dipropionato)iron; dcim = 1,5-dicyclohexylimidazole. From ref. 16. [c] From ref. 1.

The complexes **(3b)**·dmim and **(3c)**·mim bound dioxygen only at temperatures below −20 and −66 °C, respectively. Both complexes could associate and dissociate dioxygen reversibly with increasing or decreasing temperature and during this cycle no irreversible oxidation *via* a bimolecular process was obtained. Values for P_{50} were found to be independent of the wavelength used to determine the extent of dioxygenation. The data were fitted by equation (4) employed by Collman *et al.*,[14]

$$P_{O_2} = [ML]_T b\Delta\varepsilon(P_{O_2}/\Delta A) - P_{50} \quad (4)$$

where $[ML]_T$ is the total metalloporphyrin concentration, b is the cell path length, $\Delta\varepsilon$ is the difference in molar absorptivity of the oxy and deoxy complexes, and ΔA is the difference between the absorbance at the particular P_{O_2} and the absorbance of the deoxy complex at the same wavelength. Plots of P_{O_2} *vs.* $P_{O_2}/\Delta A$ gave straight lines with the y intercept being equal to $-P_{50}$. Values obtained for the dioxygenation of the complexes are shown in Table 1.

Table 1 shows also the enthalpy and entropy of the oxygenation equilibrium of the **(3b)**·dmim complex determined from van't Hoff plots, using titration data obtained at five different temperatures.

The dynamics of dioxygen binding to complex **(3b)** could be explored by laser flash photolysis. The experiment was carried out under conditions where direct rebinding according to equation (5) is believed to be occurring. The conditions where

$$ML{\cdot}B{\cdot}O_2 \xrightarrow{h\nu} ML{\cdot}B \underset{k_B^{-O_2}}{\overset{k_B^{O_2}}{\rightleftharpoons}} ML{\cdot}B{\cdot}O_2 \quad (5)$$

the rate of return to equilibrium following photolysis [$k_{obs.}$, equation (6)] was independent of axial base concentration were

$$k_{obs.} = k_B^{O_2}[O_2] + k_B^{-O_2} \quad (6)$$

determined in advance. When concentration of mim ranged from 3×10^{-2} to 3×10^{-1} mol dm^{-3} the value of $k_{obs.}/[O_2]$ was invariant, therefore dioxygen rebinding must occur prior to the second base rebinding. Under these conditions plots of log A *vs.* t are linear at high concentrations of dioxygen. This means clean monophasic rebinding. Values of $k_B^{O_2}$ and $k_B^{-O_2}$ obtained using equation 6 are shown in Table 2.

Infrared Spectra.—Difference spectra of **(3b)**·him adducts of $^{16}O_2$ *vs.* $^{18}O_2$ (90% enriched) and of CO *vs.* argon atmospheres were measured in the regions 1 200—1 000 and 2 000—1 800 cm^{-1}, respectively, at 25 °C. In the $^{16}O_2$ *vs.* $^{18}O_2$ spectra, a band at 1 166 cm^{-1} appeared and that at 1 084 cm^{-1} was lost, the shift in stretching frequencies of the $^{16}O_2$ and $^{18}O_2$ adducts of **(3b)** being in accord with Hooke's law. For the CO *vs.* argon atmospheres a new band appeared at 1 979 cm^{-1}. The i.r. data for complex **(3b)** are shown in Table 3.

Mössbauer Spectra.—Mössbauer spectra of the adducts **(3b)**·2him, **(3b)**·him·CO, and **(3b)**·him·O_2 were measured at 77 K. They were fitted by Lorentzian line shapes using a least-squares program. The isomer shift (δ) and quadrupole splitting (ΔE_Q) obtained are shown in Table 4.

Discussion

One unique feature of 'bis-fenced porphyrins', compared to sterically unprotected porphyrins (one-face protected porphyrins) is their ability to block both the axial sites of a porphyrinatoiron complex. The co-ordination of complex **(3b)** to an axial base such as an imidazole derivative is presumed to be controlled by the four pivaloyloxy fences on both sides of the porphyrin plane.

In the case of the less-hindered base mim a flat porphyrinatoiron(II) complex will bind a second base more strongly than the first one due to the accompanying electron-spin changes in going from five- to six-co-ordinate iron(II).[13] The reaction of the haem with the sterically hindered base dmim affords only a five-co-ordinated high-spin species owing to the repulsive interactions between the hydrogen atoms of the 2-methyl group and the electrons of the porphyrin ring, the iron lying outside the porphyrin plane.[15] Modified porphyrins, where the one side of the porphyrin plane is protected by bulky groups and there is an appropriate cavity around the axial co-ordination position of a metal ion, *i.e.* 'pocket',[1] 'capped',[2] 'cyclophane',[16] and

Table 3. Infrared spectral data (cm^{-1}) for iron(II) porphyrin complexes at 25 °C

Haem	Ligand	Solvent	O_2 Adduct $\nu(^{16}O-^{16}O)(\nu_{\frac{1}{2}})$	$\nu(^{18}O-^{18}O)$	CO Adduct $\nu(CO)(\nu_{\frac{1}{2}})$
(**3b**)	him	Benzene	1 166(10)	1 084	1 979(12)
[Fe(tpvp)][a]	mim	Nujol	1 159(—)	1 075	1 968
hb[b]	—	Water	1 107(9 ± 1)	1 065	1 951(8)
mb[c]	—	Water	1 103(8 ± 1)	1 065	1 944(12)
O_2 or CO gas[d]	—	—	1 556	—	2 143
O_2^-[d]	—	—	1 145	—	—

[a] From ref. 19. [b] From C. H. Barlow, J. C. Maxwell, W. J. Wallace, and W. S. Caughey, *Biochem. Biophys. Res. Commun.*, 1973, **55**, 91. [c] J. G. Maxwell, J. A. Volpe, C. H. Barlow, and W. S. Caughey, *Biochem. Biophys. Res. Commun.*, 1974, **58**, 166. [d] From ref. 20.

Table 4. Mössbauer parameters (mm s^{-1}) for iron(II) porphyrin complexes at 77 K

Haem	Ligand	Solvent	Deoxy δ	Deoxy ΔE_Q	CO Adduct δ	CO Adduct ΔE_Q	O_2 Adduct δ	O_2 Adduct ΔE_Q
(**3b**)	him	Toluene	0.44	1.00	0.27	0.32	0.25	2.02
[Fe(tpvp)][a]	mim	Toluene	0.44	0.99	0.27[b]	0.27[b]	0.27	2.04
Chelated[c]	Him	—	0.95	2.06	0.22	0.38	—	—
hb[d]	—	—	0.92[b]	2.37[b]	0.26[b]	0.26[b]	0.26	2.19
mb[d]	—	—	0.90	2.20	0.27[b]	0.36[b]	0.22	2.27

[a] From ref. 21. [b] At 4.2 K. [c] From E. Tsuchida, H. Nishide, H. Yokoyama, H. Inoue, and T. Shirai, *Polym. J.*, 1984, **16**, 325. [d] From refs. 23 and 24.

'cofacial'[17] porphyrins, permit the monoligation of unhindered bases at the axial position outside of the cap.

In this work, steric effects of the 2,6-dipivaloyl substituents attached to the phenyl ring on axial ligation were first investigated. Complex (**3b**) has two highly modulated cavities on both sides of the porphyrin plane, and so exerts a strong steric effect on the fifth and sixth co-ordination positions of the central ion. As expected, both equilibrium constants for base ligation (K^B, $K_B{}^B$) were significantly decreased in comparison to unhindered porphyrin complexes. Bis-ligated adducts are the dominant species in solution in the case of mim. The data in Table 1 show that complexes (**3b**) and (**3c**) bind bases more weakly than do 'tetraphenylporphyrins',[13] 'picket-fence porphyrins',[1] and 'bis-pocket porphyrins'.[5] This might be caused by the greater steric hindrance afforded by the bulky ester groups held rigidly around the co-ordination pockets of (**3b**) and (**3c**). It is clear that steric factors operate to decrease the size of the axial pockets available for co-ordination.

Table 1 shows many interesting features of the bis-fenced porphyrins. The adduct (**3b**)·dmim and (**3c**)·mim formed dioxygen adducts only at low temperature owing to their low oxygen affinity. Both complexes associated and dissociated dioxygen reversibly with increasing or decreasing temperature and during this cycle no irreversible oxidation *via* a bimolecular process was observed. This indicates that the bulky ester groups on both sides of the porphyrin plane impede the formation of an intermolecular μ-dioxo dimer. The value of P_{50} for (**3b**)·dmim is 15 times larger than that for (**3b**)·mim (apparent) at 25 °C. A change in the axial base from mim to dmim produces a decrease in oxygen affinity for (**3b**). This is similar to haemoglobin changing from the R to the T state. The effect of dmim is due to the steric hindrance of the 2-methyl group which resists the metal entering the porphyrin plane on deoxygenation.[15]

The P_{50} values of (**3b**)·dmim and (**3c**)·mim were low compared to those of the corresponding adducts having intermolecular polar amide residues. The low oxygen affinity of 'bis-fenced porphyrin' systems could be the result of: (1) a less polar pocket effect around the ligand-binding site including intermolecular hydrogen bonding and/or less dipole–dipole interaction between the polar fence and the bound dioxygen; (2) unfavourable steric interactions between the axial base and the ester fences. The oxygen-binding affinity of a bis-pocket porphyrin having an apolar fence was lower than that of a picket-fence porphyrin having a more polar environment.[5] Bis-fenced porphyrins do not have amide groups which can lead to hydrogen bonding with the bound dioxygen. It is assumed that the low oxygen-binding affinity of complexes (**3b**) and (**3c**) arises from the nature of the binding pocket. However the second factor for an axially substituted imidazole would predominate in determining the oxygen affinity. It is well known that electronic and steric factors influence the affinities of iron(II) porphyrins for gaseous ligands. Collman *et al.*[18] have reported a decrease in basicity of the axial base gives rise to a 40-fold reduction in oxygen affinity upon replacing imidazole by pyridine.[18]

Therefore, in the case of complex (**3b**), it appears that the unfavourable steric interaction between the axial base and the ester fence evidenced from small K^B and $K_B{}^B$ values must play a major role in the reduced oxygen-binding affinity, as in the case of chelated haem.[19]

The thermodynamic values in Table 1 show that the major difference in dioxygen binding by complex (**3b**) are manifested in the enthalpy term. The values are higher than for other metalloporphyrin systems, which means that the process of binding dioxygen to form a six-co-ordinate adduct requires less energy than in the other cases. The values of ΔS are also higher for (**3b**) than for the other metalloporphyrins, which means the loss of degrees of freedom in binding dioxygen is smaller. This indicates the formation of a rather weak dioxygen adduct. In comparison to pocket-fence porphyrins, the diminished oxygen-binding affinity of complex (**3b**) is primarily enthalpic.[14]

The kinetic data obtained in this study suggested that the lowered affinity of the bis-fenced complex is reflected by an increased dissociation rate for bound dioxygen. In the case of 'hanging-base porphyrins', Momenteau *et al.*[3] have concluded that the constraints on the proximal side greatly affect the equilibrium constant for dioxygen binding. An increase in the number of methylene carbon atoms in the chain connecting the pyridine ring to the macrocycle gave a 10-fold reduction in equilibrium constant, principally because of the large

dissociation rate. Furthermore, this group has suggested that changing the mode of attachment of the distal handles strongly modifies the oxygen affinity. It was found that the amide derivative had an affinity for dioxygen greater than did the ether analogue, according to a 10-fold reduction in the dioxygen dissociation rate for the former complex.[3] The increase in stability of the oxygenated 'amide' species is attributed to the presence of the amide residues which have the ability to undergo hydrogen bonding to the terminal oxygen atom of the ligated molecular oxygen. The kinetic results for complex (**3b**), the ester residues of which cannot have direct interaction with dioxygen, are in agreement with this suggestion. However, the high rate of dissociation of dioxygen from its adduct with (**3b**) is presumably attributed to the steric interaction between the axial base and the ester fences rather than to electrostatic interaction. It can be concluded that the pockets formed by the sterically bulky substituents around the ligand binding site reduce the affinity of dioxygen through the reduction of binding energy, resulting in a higher dissociation rate.

The ν(CO) value of the adduct (**3b**)·him (1 979 cm^{-1}) is higher than that of the complex [Fe(tpvp)]·mim [tpvp = 5,10,15,20-tetra(pivalamidophenyl)porphyrinate] (1 968 cm^{-1}).[20] This shift in stretching frequency is attributed to small π-back donation from Fe to the bound CO. This is derived from the unfavourable steric interaction between the axial base and the ester fences, causing a reduction in the π-bond character of the bound CO molecule.

The $\nu(O_2)$ value for the dioxygen adduct of (**3b**)·him complex is close to those of ionic superoxides, for which the characteristic absorption band is found at 1 150—1 100 cm^{-1}, and approximately agrees with that of the dioxygen adduct of [Fe(tpvp)]·mim.[21] The small shift in $\nu(O_2)$ of (**3b**)·him in comparison with [Fe(tpvp)]·mim shows the difference in the local environment of the binding site and the ligation characteristics of a proximal base. As noted above, ν(CO) is mainly affected by the nature of the ligation of the axial base. However, this correlation fails to hold in dioxygen complexes, because other effects such as hydrogen bonding and dipole–dipole interaction may affect the resonance frequency of the bound dioxygen.

Mössbauer parameters at 77 K for the deoxy, CO, and oxy complexes of (**3b**) are summarized in Table 4. For the deoxy (**3b**)·2him complex, both δ and ΔE_Q were small and nearly equal to those of [Fe(tpvp)]·2mim, indicating that the iron was in the +II low-spin state.[22] For the CO adduct of (**3b**), both δ and ΔE_Q were smaller than those of the deoxy complex owing to a π-back donation to the co-ordinated CO. Furthermore, ΔE_Q was a little larger than that of [Fe(tpvp)]·mim·CO because of a large electric field gradient at the iron nucleus. This indicates that the binding of an axial base to the sixth co-ordination site undergoes steric interference by the bulky ester fences. The fact that the value of ν(CO) shifted to higher wavenumber, as mentioned above, is also in agreement with this.

For the dioxygen adducts of complex (**3b**) the Mössbauer parameters were consistent with those of oxy-haemoglobin and myoglobin. The small δ value and large ΔE_Q value for the dioxygen adduct mean that the iron ion is in a +III low-spin state. This suggests a charge-separated structure Fe^{III}–O_2^- which has been reported for oxyhaemaglobin and [Fe(tpvp)]·mim·O_2.[23,24] It is interesting that the Mössbauer parameters of (**3b**)·him·O_2 are extremely close to those of [Fe(tpvp)]·mim·O_2, while less similarity was observed for the CO complexes.

In conclusion, a new methodology is presented in this paper for the synthesis of both-faces-hindered porphyrin complexes which is much simpler and gives higher yields in comparison with previous methods. The highly symmetrical 5,10,15,20-tetra(2′,6′-dipivaloyloxyphenyl)porphyrin removed the complexity of diastereoisomeric properties. The iron(II) and cobalt(II) complexes quantitatively showed the steric effects of the bulky fences on both sides of the porphyrin plane when binding nitrogen-containing ligands and dioxygen. The ester fences without amide groups on both sides of the macrocycle resulted in dioxygen adducts stable to irreversible oxidation at 25 °C in toluene. This indicates that an electrostatic interaction between the fence groups and the bound dioxygen is not essential to the formation of a dioxygen adduct.

Acknowledgements

The authors thank Dr. Hidenari Inoue of Keio University for the measurement of Mössbauer spectra. This work was partially supported by a Grant-in-Aid for Scientific Research on Priority Area 'Macromolecular Complexes' from the Ministry of Education, Science and Culture.

References

1 J. P. Collman, R. R. Gagne, C. A. Reed, T. R. Halbert, G. Lang, and W. T. Robinson, *J. Am. Chem. Soc.*, 1975, **97**, 1427; J. P. Collman, J. I. Brauman, B. L. Iverson, J. L. Sessler, R. M. Morris, and Q. H. Gibson, *ibid.*, 1983, **105**, 3052.
2 J. E. Linad, P. E. Ellis, jun., J. R. Budge, R. D. Jones, and F. Basolo, *J. Am. Chem. Soc.*, 1980, **102**, 1896.
3 M. Momenteau, B. Loock, C. Tetreau, D. Lavalette, A. Croisy, C. Schaeffer, C. Huel, and J. M. Lhoste, *J. Chem. Soc., Perkin Trans. 2*, 1987, 249; M. Momenteau, *Pure Appl. Chem.*, 1986, **58**, 1493.
4 C. K. Chang and T. G. Traylor, *Proc. Natl. Acad. Sci. USA*, 1975, **72**, 1166.
5 K. S. Suslick and M. M. Fox, *J. Am. Chem. Soc.*, 1983, **105**, 3507.
6 E. Tsuchida, H. Nishide, M. Yuasa, E. Hasegawa, and Y. Matsushita, *J. Chem. Soc., Dalton Trans.*, 1984, 1147; E. Tsuchida, H. Nishide, M. Yuasa, E. Hasegawa, Y. Matsushita, and K. Eshima, *ibid.*, 1985, 275; M. Yuasa, H. Nishide, and E. Tsuchida, *ibid.*, 1987, 2493.
7 A. R. Battersby, S. A. J. Bartholomew, and T. Nitta, *J. Chem. Soc., Chem. Commun.*, 1983, 1291.
8 J. E. Baldwin and J. Huff, *J. Am. Chem. Soc.*, 1973, **95**, 5757; J. Almog, J. E. Baldwin, and J. Huff, *ibid.*, 1975, **97**, 227; J. E. Baldwin, J. H. Cameron, M. J. Crossly, I. J. Dagley, and T. Klose, *J. Chem. Soc., Dalton Trans.*, 1984, 1739.
9 B. Shaanan, *Nature (London)*, 1982, **296**, 683.
10 I. P. Gerothanassis, M. Momenteau, and B. Loock, *J. Am. Chem. Soc.*, 1989, **111**, 7006.
11 T. Komatsu, E. Hasegawa, H. Nishide, and E. Tsuchida, *J. Chem. Soc., Chem. Commun.*, 1990, 66.
12 R. S. Drago, 'Physical Methods in Chemistry,' W. B. Saunders, Philadelphia, 1977, p. 88.
13 D. Brault and M. Rougee, *Biochem. Biophys. Res. Commun.*, 1974, **57**, 654.
14 J. P. Collman, J. I. Brauman, K. M. Doxsee, T. R. Halbert, S. E. Hayes, and K. S. Suslick, *Proc. Natl. Acad. Sci. USA*, 1978, **75**, 564.
15 J. B. Jameson, F. S. Malinaro, J. A. Ibers, J. P. Collman, J. I. Brauman, E. Rose, and K. S. Suslick, *J. Am. Chem. Soc.*, 1980, **100**, 3224.
16 T. G. Traylor, M. J. Mitchell, S. Tsuchiya, D. H. Campbell, D. V. Stynes, and N. Koga, *J. Am. Chem. Soc.*, 1981, **103**, 5234.
17 B. Ward, C. B. Wang, and C. K. Chang, *J. Am. Chem. Soc.*, 1981, **103**, 5236.
18 J. P. Collman, J. I. Brauman, K. M. Doxsee, J. L. Sessler, R. M. Morris, and Q. H. Gibson, *Inorg. Chem.*, 1983, **22**, 1427.
19 J. Geibel, J. Caanon, D. Campbell, and T. G. Traylor, *J. Am. Chem. Soc.*, 1978, **100**, 3575; T. G. Traylor, *Acc. Chem. Res.*, 1981, **14**, 102.
20 J. P. Collman, J. I. Brauman, T. R. Halbert, and K. S. Suslick, *Proc. Natl. Acad. Sci. USA*, 1976, **73**, 33.
21 J. C. Evans, *Chem. Commun.*, 1969, 682.
22 K. Spartalian, G. Lang, J. P. Collman, R. R. Gagne, and C. A. Reed, *J. Chem. Phys.*, 1975, **63**, 5375.
23 G. Lang and W. Marshall, *Proc. Phys. Soc. London*, 1966, **87**, 3.
24 K. Spartalian, G. Lang, and T. Yonetani, *Biochem. Biophys. Acta*, 1976, **428**, 281.

Received 26*th March* 1990; *Paper* 0/00459F